ACS Macro Letters
Letter
pubs.acs.org/macroletters

Synthesis and Effect of Physical Aging on Gas Transport Properties of a Microporous Polyimide Derived from a Novel Spirobifluorene-Based Dianhydride

Xiaohua Ma, Bader Ghanem, Octavio Salines, Eric Litwiller, and Ingo Pinnau*

Advanced Membranes and Porous Materials Center, Division of Physical Sciences and Engineering, King Abdullah University of Science and Technology (KAUST), Thuwal 23955, KSA

Ⓢ *Supporting Information*

ABSTRACT: A novel generic method is reported for the synthesis of a spirobifluorene-based dianhydride (SBFDA). An intrinsically microporous polyimide was obtained by polycondensation reaction with 3,3′-dimethylnaphthidine (DMN). The corresponding polymer (SBFDA-DMN) exhibited good solubility, excellent thermal stability, as well as significant microporosity with high BET surface area of 686 m^2/g. The O_2 permeability of a methanol-treated and air-dried membrane was 1193 Barrer with a moderate O_2/N_2 selectivity of 3.2. The post-treatment history and aging conditions had great effects on the membrane performance. A significant drop in permeability coupled with an increase in selectivity was observed after long-term aging. After storage of 200 days, the gas separation properties of SBFDA-DMN were located slightly above the latest Robeson upper bounds for several gas pairs such as O_2/N_2 and H_2/N_2.

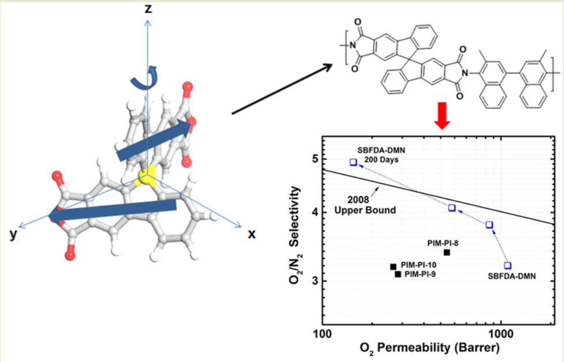

Membrane-based gas separation has great commercial potential in a variety of industrial fields, such as hydrogen recovery (H_2/N_2), on-site nitrogen production, and oxygen enrichment (O_2/N_2) as well as emerging applications in natural gas sweetening (CO_2/CH_4, H_2S/CH_4) and flue gas treatment (CO_2/N_2).[1−4] An ideal membrane is characterized by both high permeability and selectivity. However, commercial membranes used in industrial gas separation processes typically exhibit only moderate permeability and selectivity.[2,4] Generally, in glassy polymer membranes, there is a trade-off between the permeability (P) and selectivity (α), first proposed and updated by Robeson[5,6] and theoretically analyzed by Freeman.[7] This trade-off provides performance criteria for evaluation of newly developed polymer membranes.

Rational molecular design provides an efficient way for development of new polymers for advanced gas separation membranes with superior performance. The introduction of micropores (<20 Å) and, especially ultramicropores (<7 Å), to form polymers of intrinsic microporosity (PIM) can substantially enhance gas transport performance. The prototype polymer of intrinsic microporosity (PIM-1) was first reported by McKeown and Budd in 2004.[8,9] PIM-1 is a ladder polymer with fused rings linked by a spirobisindane center, which provides an intrachain contortion site that leads to inefficient chain packing and gives rise to considerable free volume. In addition, amorphous PIM-1 is soluble in common solvents such as THF and $CHCl_3$ and, therefore, can easily be solution processed to form membranes which exhibit transport properties that surpass the permeability/selectivity upper bounds for some gas pairs.[10−12] Extensive investigations have been applied to the prototype PIM-1 and its analogues.[13−26] Significant improvements were obtained by recently developed triptycene-based A−B type (TPIM-1 and TPIM-2) and Tröger's base-based ladder polymers, which exhibited outstanding gas separation performance for O_2/N_2, H_2/N_2, and H_2/CH_4 separation with properties well above the latest 2008 Robeson trade-off curves.[27,28]

The concept of polyimides of intrinsic microporosity (PIM-PI) was introduced by McKeown's group in 2008.[29−31] PIM-PIs made from spirobisindane-based dianhydrides (SBIDA) exhibited remarkably enhanced permeability compared to conventional low-free-volume polyimides. The most permeable PIM−PIs were obtained by polycondensation of extended (PIM-PI-8) and nonextended SBIDA (PIM-PI-10) with 3,3′-dimethylnaphthidine (DMN), a bulky, sterically hindered diamine.[29,31] However, the performance of these polyimides (Figure 1) fell below the 2008 Robeson upper bounds because of their low to moderate selectivities.

On the other hand, PIM-PIs made from dianhydrides with bridged bicyclic contortion sites showed significantly improved gas separation performance. Rogan et al. reported a novel ethanoanthracene dianhydride (EADA), and the polyimide made with DMN (PIM-PI-12; Figure 1) surpassed the latest permeability/selectivity trade-off curves after long-term aging.[32]

Received: January 2, 2015
Accepted: January 25, 2015
Published: January 29, 2015

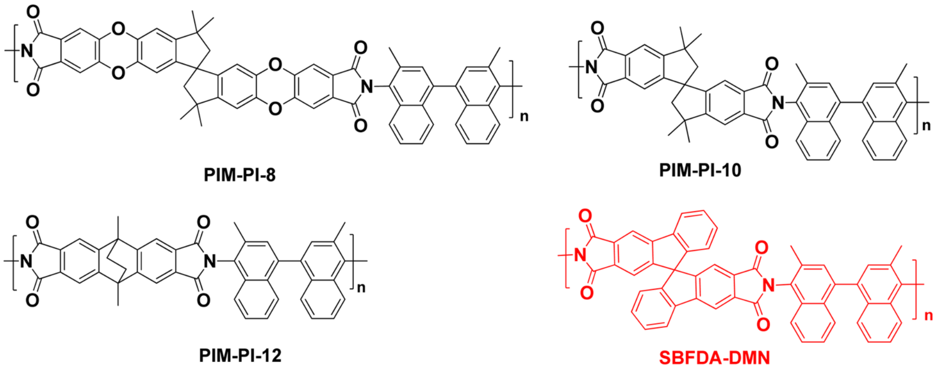

Figure 1. Structures of polyimides of intrinsic microporosity: SBIDA-DMN (PIM-PI-8, PIM-PI-10), EADA-DMN (PIM-PI-12), and SBFDA-DMN (this study).

Scheme 1. Synthetic Procedure of Spirobifluorene Dianhydride (SBFDA) and PIM-PI (SBFDA-DMN)

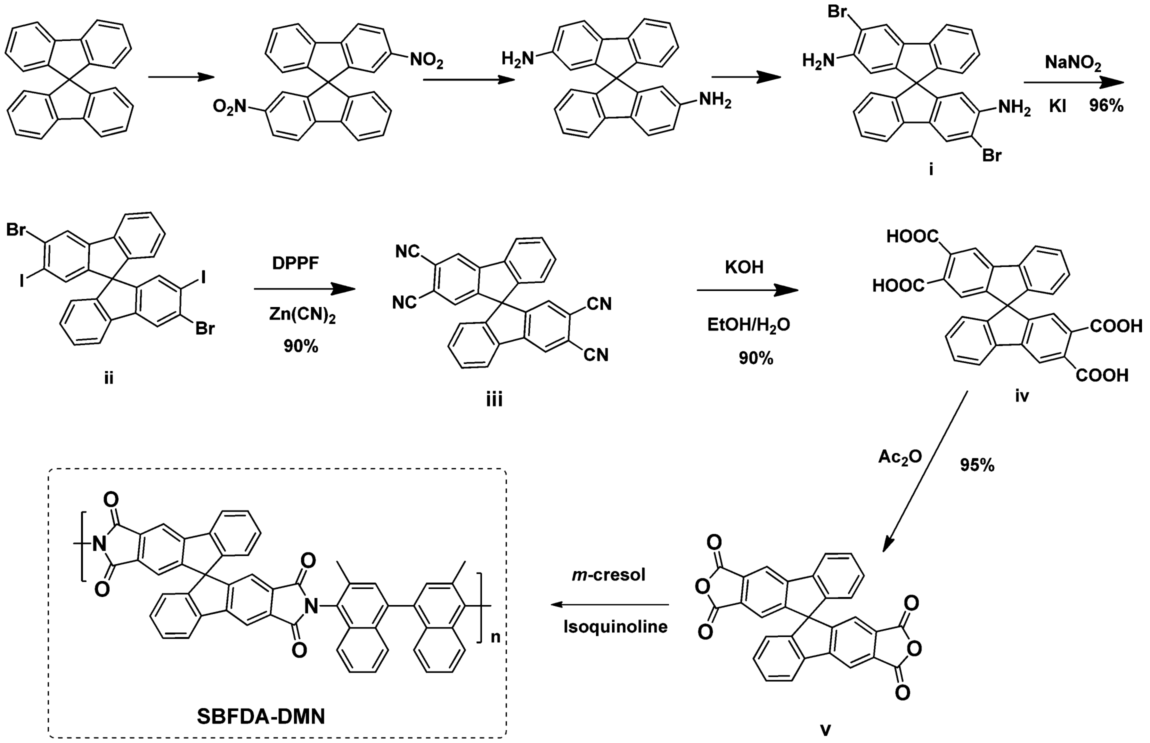

Recently, our group reported a series of 9,10-diisopropyl-triptycene dianhydride-based polyimides, which significantly outperformed the latest upper bound for several gas pairs by strong size-sieving properties due to their ultramicroporous structure.[33,34] Although these results are very encouraging, further developments of new PIM-PIs have been limited by the availability of only a few sterically hindered and contorted dianhydrides.

Here, we report the synthesis and gas separation properties of a DMN-based PIM-PI made from a novel spirobifluorene dianhydride (SBFDA). The detailed synthetic procedure is shown in Scheme 1.

First, the 3,3′-dibromospirobifluorene-2,2′-diamine (**i**), obtained as reported in our previous study,[35] was converted to 3,3′-dibromo-2,2′-diiodo-spirobifluorene (**ii**) via the Sandmeyer reaction in high yield. The intermediate **ii** was then converted to intermediate (**iii**) by the Rosenmund−von Braun reaction in the presence of a catalytic amount of tris(dibenzylideneacetone)dipalladium ($Pd_2(dba)_3$) and 1,1′-bis(diphenylphosphino)ferrocene (DPPF) to 2,2′,3,3′-tetracyano-9,9′-spirobifluorene under mild conditions.[36] Intermediate **iii** was further hydrolyzed and thereafter refluxed with acetic anhydride yielding the spirobifluorene-based dianhydride (**v**). The overall yield of the four steps was 74%. By cycloimidization condensation reaction of SBFDA with 3,3′-dimethylnaphthidine in *m*-cresol containing a catalytic amount of isoquinoline the polyimide SBFDA-DMN was obtained. The structure of the polymer and intermediates was fully characterized, and the details are provided in the Supporting Information.

SBFDA-DMN is readily soluble in common solvents such as NMP, DMF, *m*-cresol, and chloroform. The polymer exhibits high average molecular weight M_n of 6.5 × 10^4 g/mol and narrow polydispersity with PDI of 1.92, as tested by GPC using chloroform as eluent (Table 1). In addition, SBFDA-DMN demonstrated very good thermal stability as illustrated in Figure S1 (Supporting Information); the onset decomposition temperature was 520 °C, and the charcoal yield was about 70% at 800 °C under N_2 atmosphere; furthermore, no glass

Table 1. Basic Properties of SBFDA-DMN

polymer	$M_n \times 10^{-4}$ (g/mol)[a]	PDI	T_d (°C)	S_{BET} (m^2/g)
SBFDA-DMN	6.5	1.92	520	686 (608)[b]

[a] Measured by GPC using chloroform as solvent with polystyrene as external standard. The rate of the eluent speed was 1 mL/min. [b] Based on nitrogen adsorption on powder at 77 K; in the brackets is the BET surface area of SBFDA-DMN aged for 200 days.

transition temperature was observed up to 400 °C by DSC (Figure S2, Supporting Information).

Because of the rigid 90° contortion center of the spirobifluorene moiety, SBFDA-DMN exhibits significant microporosity as illustrated by its N_2 adsorption/desorption isotherms (Figure 2a). SBFDA-DMN showed large nitrogen uptake at very low relative pressure ($p/p_0 < 0.05$), indicating the presence of a significant fraction of micropores below 20 Å. After aging under ambient conditions for 200 days, SBFDA-DMN showed a 12% drop in BET surface area from 686 to 608 m^2/g. The pore size distributions below 20 Å of the freshly made and aged sample were analyzed using the DFT model and are shown in Figure 2b. It is interesting to note that SBFDA-DMN contains a large amount of ultramicropores (<7 Å) and pores larger than 1 nm in both the freshly made and aged polymer samples, with a remarkable increase in the number of ultramicropores due to shrinkage of pores larger than 10 Å after aging for 200 days. However, freshly made and aged membrane samples showed essentially the same halo and *d*-spacing (6.4 Å), as determined by WAXD (Figure S3, Supporting Information).

The pure-gas permeability of SBFDA-DMN for H_2, N_2, O_2, CH_4, and CO_2 was determined by the constant-volume/variable-pressure method, and the results are summarized in Table 2. According to a previously reported post-treatment method to remove trace amounts of chloroform from the porous texture of PIM-PIs,[27,32] a freshly made SBFDA-DMN membrane (123 μm thick, cast from chloroform) was soaked in methanol and thereafter air-dried for 1 day. Like other DMN-based PIM-PIs, a SBFDA-treated membrane based on such protocol showed very high gas permeabilities. For example, a freshly made and methanol-treated SBFDA-DMN membrane had an O_2 permeability of 1193 Barrer with a moderate O_2/N_2 selectivity of 3.2. The order of gas permeabilities was similar to that of other high free volume PIMs and PIM-PIs, that is, $PCO_2 > PH_2 > PO_2 > PCH_4 > PN_2$. The differences in selectivity between freshly made SBFDA-DMN, SBIDA-DMN, (PIM-PI-8; PIM-PI-10), and EADA-DMN (PIM-PI-12) membranes were relatively small. It is important to note that the membrane drying conditions and aging time had a critical effect on the performance of SBFDA-DMN, as shown in Table 2.

Drying the polymer at 120 °C after methanol treatment and extended aging time resulted in a significant decrease in gas permeability coupled with a large increase in selectivity for all gas pairs. For example, the O_2 permeability dropped 7-fold from 1193 to 161 Barrer after heat treatment at 120 °C and storage of 200 days, whereas the O_2/N_2 selectivity increased from 3.2 to 4.9. Upon physical aging, the increase in permselectivity can be attributed to an increase in the diffusion selectivity (Table S1, Supporting Information). This result is qualitatively consistent with previously reported gas permeation data for other aged PIM-PIs, such as the bridged bicyclic EADA-DMN (PIM-PI-12) and triptycene dianhydride-based PIM-PIs.[32−34] The densification of the microporous SBFDA-DMN structure is also evident by the reversal of the order of the H_2 vs CO_2 permeability upon aging over 200 days (Table 2). This result is in agreement with the DFT pore size distribution analysis of the fresh and aged samples discussed above. The long-term aging data indicate clearly that PIM-PIs are far from their equilibrium physical state when methanol-treated and tested shortly after film formation. Hence, it is desirable for future studies to develop protocols that facilitate the physical aging process of glassy PIM-PIs to obtain more realistic “intrinsic” gas permeation data. The gas separation properties of SBFDA-DMN and other previously reported PIM-PIs for O_2/N_2 and H_2/N_2 are shown on the 2008 Robeson upper bounds in Figure 3.

Similar qualitative behavior was observed between SBFDA-DMN and PIM-PI-12; that is, long-term physical aging resulted in loss of permeability with a concurrent increase in selectivity that boosted the performance of both polymers over the upper bound lines for O_2/N_2 and H_2/N_2 separation.

In summary, a generic method for synthesis of a spirobifluorene dianhydride is reported. An intrinsically microporous polyimide with high BET surface area was obtained by polycondensation reaction of SBFDA with DMN. The polyimide exhibited good solubility, excellent thermal stability, and significant microporosity. A methanol-treated and air-dried SBFDA-DMN membrane showed very high permeability and modest selectivity benefiting high free volume due to the contorted spirobifluorene center and the rigidity of the polymer. After thermal treatment at 120 °C and 200 day long-term physical aging, the membrane exhibited significant

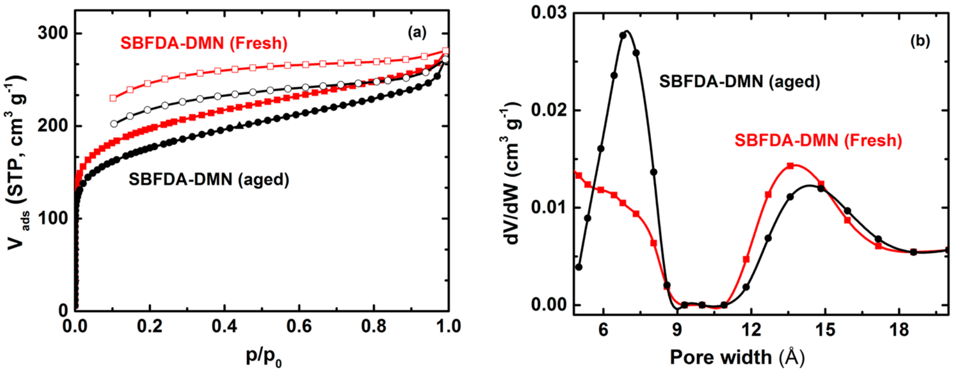

Figure 2. (a) N_2 adsorption (closed symbols)/desorption (open symbols) isotherms of freshly synthesized and aged SBFDA-DMN powder at 77 K. (b) Pore size distribution (PSD) of SBFDA-DMN below 2 nm analyzed by the DFT model using N_2 as a probe.

Table 2. Permeability and Selectivity of SBFDA-DMN (35 °C) and Other DMN-Based PIM-Polyimides (25 °C)[a]

	permeability (Barrer)					ideal selectivity (α)			
polymer	H_2	N_2	O_2	CH_4	CO_2	H_2/N_2	H_2/CH_4	O_2/N_2	CO_2/CH_4
SBFDA-DMN[b]	3342	369	1193	581	6674	9.1	5.8	3.2	11.5
SBFDA-DMN[c]	2966	226	850	326	4700	13.1	9.1	3.8	14.4
SBFDA-DMN[d]	2146	143	593	199	3049	15.0	10.8	4.1	15.3
SBFDA-DMN[e]	878	33	161	40	703	26.6	22.0	4.9	17.6
PIM-PI-8[f]	1600	160	545	260	3700	10.0	6.2	3.4	14.2
PIM-PI-10[g]	2560	340	1010	550	5190	7.5	4.7	3.0	9.4
PIM-PI-12[h]	4230	369	1380	457	6340	11.5	9.3	3.7	13.9
PIM-PI-12[i]	2860	131	659	156	3230	21.8	18.3	5.0	20.7

[a] All polyimide membranes cast from $CHCl_3$. [b] SBFDA-DMN soaked in methanol and then air-dried for 24 h. [c] SBFDA-DMN soaked in methanol and then dried at 120 °C under vacuum for 24 h. [d] Sample b tested after 10 days. [e] sample b tested after 200 days. [f] PIM-PI-8 dried at ambient temperature, data from ref 29. [g] PIM-PI-10 soaked in methanol and dried at ambient temperature, data from ref 31. [h] PIM-PI-12 soaked in methanol and dried at ambient temperature, data from ref 32. [i] Sample g tested after 273 days.

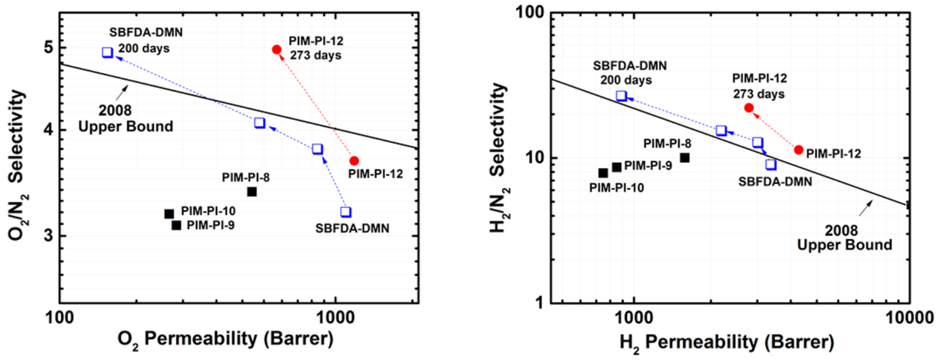

Figure 3. Robeson plots of SBFDA-DMN (blue squares and line for aging trend from freshly made sample to 200 days of storage), spirobisindane-based PIM-PI-8, 9, and 10 (black squares), and ethanoanthrancene-based PIM-PI-12 (red dots and line for aging trend from freshly made sample to 273 days of storage) microporous polyimides for O_2/N_2 and H_2/N_2 gas pairs.

lower permeability with enhanced selectivity and surpassed the upper bounds for O_2/N_2 and H_2/N_2 gas pairs.

■ ASSOCIATED CONTENT

Ⓢ Supporting Information

The detailed synthetic procedure and characterization of the polymer and intermediates, TGA, DSC, WAXD of the polymer, membrane formation protocol, gas permeation measurement technique and gas transport data are reported. This material is available free of charge via the Internet at http://pubs.acs.org.

■ AUTHOR INFORMATION

Corresponding Author

*E-mail: ingo.pinnau@kaust.edu.sa.

Notes

The authors declare no competing financial interest.

■ ACKNOWLEDGMENTS

This work was supported by KAUST funding for Prof. Ingo Pinnau.

■ REFERENCES

(1) Bernardo, P.; Drioli, E.; Golemme, G. *Ind. Eng. Chem. Res.* **2009**, *48*, 4638.
(2) Baker, R. W.; Lokhandwala, K. *Ind. Eng. Chem. Res.* **2008**, *47*, 2109.
(3) Baker, R. W.; Low, B. T. *Macromolecules* **2014**, *47*, 6999.
(4) Baker, R. W. *Ind. Eng. Chem. Res.* **2002**, *41*, 1393.
(5) Robeson, L. M. *J. Membr. Sci.* **1991**, *62*, 165.
(6) Robeson, L. M. *J. Membr. Sci.* **2008**, *320*, 390.
(7) Freeman, B. D. *Macromolecules* **1999**, *32*, 375.
(8) Budd, P. M.; Elabas, E. S.; Ghanem, B. S.; Makhseed, S.; McKeown, N. B.; Msayib, K. J.; Tattershall, C. E.; Wang, D. *Adv. Mater.* **2004**, *16*, 456.
(9) Budd, P. M.; Ghanem, B. S.; Makhseed, S.; McKeown, N. B.; Msayib, K. J.; Tattershall, C. E. *Chem. Commun.* **2004**, 230.
(10) Budd, P.; Msayib, K.; Tattershall, C.; Ghanem, B.; Reynolds, K.; McKeown, N.; Fritsch, D. *J. Membr. Sci.* **2005**, *251*, 263.
(11) Budd, P.; McKeown, N.; Ghanem, B.; Msayib, K.; Fritsch, D.; Starannikova, L.; Belov, N.; Sanfirova, O.; Yampolskii, Y.; Shantarovich, V. *J. Membr. Sci.* **2008**, *325*, 851.
(12) Thomas, S.; Pinnau, I.; Du, N.; Guiver, M. D. *J. Membr. Sci.* **2009**, *333*, 125.
(13) Du, N.; Robertson, G. P.; Song, J.; Pinnau, I.; Thomas, S.; Guiver, M. D. *Macromolecules* **2008**, *41*, 9656.
(14) Du, N.; Robertson, G. P.; Pinnau, I.; Guiver, M. D. *Macromolecules* **2009**, *42*, 6023.
(15) Ma, X.; Swaidan, R.; Belmabkhout, Y.; Zhu, Y.; Litwiller, E.; Jouiad, M.; Pinnau, I.; Han, Y. *Macromolecules* **2012**, *45*, 3841.
(16) Du, N.; Robertson, G. P.; Song, J.; Pinnau, I.; Guiver, M. D. *Macromolecules* **2009**, *42*, 6038.
(17) Du, N.; Robertson, G. P.; Pinnau, I.; Guiver, M. D. *Macromolecules* **2010**, *43*, 8580.
(18) Du, N.; Park, H. B.; Robertson, G. P.; Dal-Cin, M. M.; Visser, T.; Scoles, L.; Guiver, M. D. *Nat. Mater.* **2011**, *10*, 372.
(19) Du, N.; Dal-Cin, M. M.; Pinnau, I.; Nicalek, A.; Robertson, G. P.; Guiver, M. D. *Macromol. Rapid Commun.* **2011**, *32*, 631.
(20) Carta, M.; Msayib, K. J.; Budd, P. M.; McKeown, N. B. *Org. Lett.* **2008**, *10*, 2641.
(21) Carta, M.; Msayib, K. J.; McKeown, N. B. *Tetrahedron Lett.* **2009**, *50*, 5954.

(22) Fritsch, D.; Bengtson, G.; Carta, M.; McKeown, N. B. *Macromol. Chem. Phys.* **2011**, *212*, 1137.

(23) Short, R.; Carta, M.; Bezzu, C. G.; Fritsch, D.; Kariuki, B. M.; McKeown, N. B. *Chem. Commun.* **2011**, *47*, 6822.

(24) Bezzu, C. G.; Carta, M.; Tonkins, A.; Jansen, J. C.; Bernardo, P.; Bazzarelli, F.; McKeown, N. B. *Adv. Mater.* **2012**, *24*, 5930.

(25) Vile, J.; Carta, M.; Bezzu, C. G.; Kariuki, B. M.; McKeown, N. B. *Polymer* **2014**, *55*, 326.

(26) Ghanem, B. S.; McKeown, N. B.; Budd, P. M.; Fritsch, D. *Macromolecules* **2008**, *41*, 1640.

(27) Carta, M.; Malpass-Evans, R.; Croad, M.; Rogan, Y.; Jansen, J. C.; Bernardo, P.; Bazzarelli, F.; McKeown, N. B. *Science* **2013**, *339*, 303.

(28) Ghanem, B. S.; Swaidan, R.; Ma, X.; Litwiller, E.; Pinnau, I. *Adv. Mater.* **2014**, *26*, 6661.

(29) Ghanem, B. S.; McKeown, N. B.; Budd, P. M.; Selbie, J. D.; Fritsch, D. *Adv. Mater.* **2008**, *20*, 2766.

(30) Ghanem, B. S.; McKeown, N. B.; Budd, P. M.; Al-Harbi, N. M.; Fritsch, D.; Heinrich, K.; Starannikova, L.; Tokarev, A.; Yampolskii, Y. *Macromolecules* **2009**, *42*, 7881.

(31) Rogan, Y.; Starannikova, L.; Ryzhikh, V.; Yampolskii, Y.; Bernardo, P.; Bazzarelli, F.; Jansen, J. C.; McKeown, N. B. *Polym. Chem.* **2013**, *4*, 3813.

(32) Rogan, Y.; Malpass-Evans, R.; Carta, M.; Lee, M.; Jansen, J. C.; Bernardo, P.; Clarizia, G.; Tocci, E.; Friess, K.; Lanc, M.; McKeown, N. B. *J. Mater. Chem. A* **2014**, *2*, 4874.

(33) Ghanem, B. S.; Swaidan, R.; Litwiller, E.; Pinnau, I. *Adv. Mater.* **2014**, *22*, 3688.

(34) Swaidan, R.; Al-Saeedi, M.; Ghanem, B.; Litwiller, E.; Pinnau, I. *Macromolecules* **2014**, *47*, 5104.

(35) Ma, X.; Salinas, O.; Litwiller, E.; Pinnau, I. *Macromolecules* **2013**, *46*, 9618.

(36) Iqbal, Z.; Lyubimtsev, A.; Hanack, M. *Synlett* **2008**, 2287.